

## CUMULATIVE PLASTIC STRAIN AND THRESHOLD STRESS OF A QUASI-SATURATED COMPACTED SILTY CLAY

J.T. Shahu<sup>1</sup>, Yudhbir<sup>2</sup> and S. Hayashi<sup>3</sup>

**ABSTRACT:** The knowledge of cumulative plastic strain and stability threshold of subgrade soil under cyclic loading is of prime importance in a proper design and maintenance planning of highway pavement structures and railway tracks. The soil beneath a pavement or a track usually exists under quasi-saturated conditions wherein the water voids in the soil remain continuous. Quasi-saturated specimens are essentially partially saturated at low confining pressures. However, with the increase in confining stresses, the air voids in the quasi-saturated specimens are dissolved into solution and the soil behaves like saturated material. Both monotonic and cyclic undrained triaxial tests have been carried out on quasi-saturated compacted specimens of a silty clay. The monotonic tests have been used to develop critical state soil mechanics framework for quasi-saturated behavior. The cyclic undrained behavior of quasi-saturated specimens has been then interpreted using this critical state framework. A generalized bilinear log-log model is proposed for the prediction of cumulative plastic strain with number of load cycles for fine-grained soils. Threshold stress is evaluated using both plastic strain development and pore pressure generation criteria. A generalized relationship between threshold stress ratio and plasticity index is proposed for a variety of soils at low and relatively high confining stresses.

**Keywords:** Cohesive soil, compaction, effective stress, laboratory test, pavement, deformation, repeated load

### INTRODUCTION

The knowledge of cumulative plastic strain and stability threshold of subgrade soil under cyclic loading is of prime importance in proper design and maintenance planning of highway pavement structures and railway tracks. The soil beneath a pavement or a track may be in its natural undisturbed state or be compacted depending on whether the section of pavement or track is in 'cut' or 'fill' area. In 'fill' area, soil compaction is generally done at or around optimum moisture content where most soils exist in quasi-saturated conditions (i.e., water voids are known to be continuous). Quasi-saturated conditions also prevail in 'cut' ground where the ground water table is fairly near the ground surface as that exists in lowland areas (refer Rankine's lecture by Brown, 1996). Hence, the evaluation of cumulative plastic strain and threshold stress of quasi-saturated soils under cyclic loading holds special interest to geotechnical engineers especially those associated with highway pavements and railway tracks in lowland areas.

Based on a detailed study on unsaturated tropical lateritic and saprolitic soils in both compacted and

undisturbed states, Cruz (1985) suggested that the value of pore-air pressure will be close to zero for high degrees of saturation (in general above 85% and in some soils above 90%). Under these conditions, the air voids will be occluded and the water voids will be continuous. This state of soil was termed as 'quasi-saturated' because the engineering behavior of soil in this state was found quite similar to its behavior in the saturated state. A detailed investigation by Shahu et al. (1999) revealed that at low confining pressure values, quasi-saturated specimens remain essentially partially saturated. However, with the increase in confining stresses to a level that normally exist in engineering problems, the air voids in the quasi-saturated specimens are dissolved into solution and the soil behaves like saturated material.

The degree of unsaturation is generally divided into four different zones, namely, boundary effect zone, primary transition zone, secondary transition zone and residual zone (Vanapalli et al., 1996). The characteristic feature of the boundary effect zone is the presence of continuous water voids and some occluded air voids. The beginning of the primary transition zone is marked by the presence of a suction value in soil specimens

---

<sup>1</sup> IALT life member, Indian Institute of Technology, Delhi, INDIA

<sup>2</sup> Department of Civil Engineering, Indian Institute of Technology, Kanpur, INDIA

<sup>3</sup> IALT life member, Institute of Lowland Technology, Saga University, JAPAN

*Note:* Discussion on this paper is open until June 2009

equal to the air entry value at which air enters into the largest pore of the soil. The secondary transition zone is noticed by the presence of large air voids and a significant reduction in water voids. The residual zone is evident by the soil response wherein a large increase in suction is required for a small change in water content. The quasi-saturated state represents the boundary effect zone in this classification.

In this paper, both monotonic and cyclic undrained triaxial test results on quasi-saturated compacted specimens of a silty clay have been presented. Two types of monotonic and cyclic undrained triaxial tests were conducted. In the first type, the response of the specimen was examined under low effective confining stresses by saturating the specimen using back-pressure. In the second type, the specimen was evaluated under high effective confining stresses which were obtained by raising the cell pressure up to a value where air voids are dissolved and soil behaves like saturated material. The monotonic tests have been used to develop critical state soil mechanics framework for quasi-saturated behavior. The cyclic undrained behavior of quasi-saturated specimens has been then interpreted using this critical state framework.

A generalized bilinear log-log model is proposed for the prediction of cumulative plastic strain with number of load cycles for fine grained soils. Threshold stress is evaluated using both plastic strain development and pore pressure generation criteria. The guidelines for estimating threshold stress ratio at different confining stresses are given.

## TEST DETAILS

Tests were carried out on compacted specimens of 38 mm diameter and 76 mm high alluvial silty clay described herein as Gangetic silt [plastic limit,  $w_p = 14\%$ ; plasticity index,  $I_p = 14$ ; specific gravity,  $G = 2.65$ ; clay content ( $< 2\mu$ ) = 18.5%; silt content ( $< 0.06$  mm) = 74.5%; sand content ( $> 0.06$  mm) = 7.0%; Optimum Moisture Content, OMC = 14.0%; and maximum dry density = 18.85 kN/m<sup>3</sup>]. Compaction was done in 3 layers using 25 number of blows per layer of 40 lbs (18.1 kg) Harvard miniature compactor in split spoon mould. Figures 1(a) and (b) show the water content,  $w$  versus dry density,  $\gamma_d$  relationship and particle size distribution for this soil. Tests were conducted in a commercially available Geotechnical Digital System (GDS). The equipment consists of three computer controlled piston-motor devices with inbuilt sensors for stress control, a pore pressure transducer, and a triaxial cell. Axial and radial stresses are applied

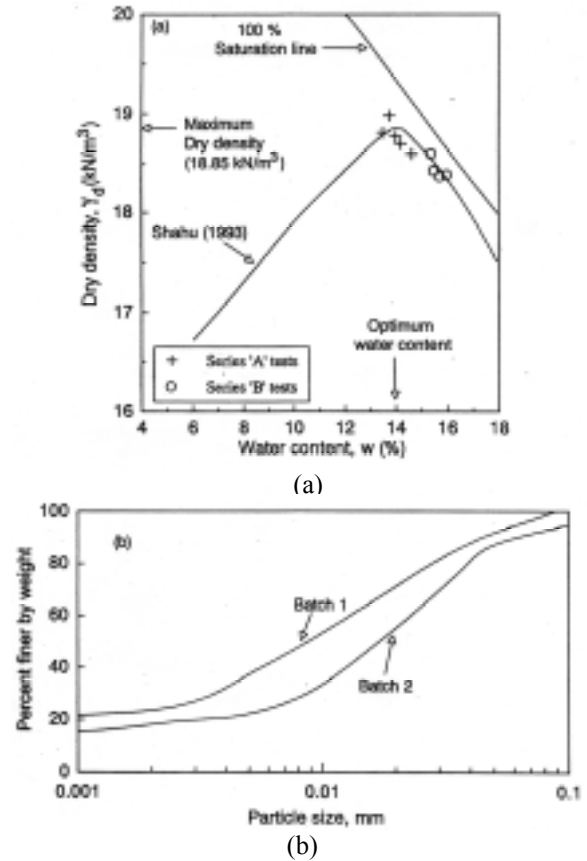


Fig.1 Basic properties of Gangetic silt: (a) water content-dry density relationship; (b) particle size distribution

hydraulically and measured using piston-motor devices. Axial deformation is automatically obtained from the recorded data of the exact piston movement. The equipment has facilities for both stress path controlled and cyclic triaxial testing. In all tests, the pore water pressure was measured at the bottom end of the specimen. The effective confining stress at any given stage of the test was calculated as the difference between the cell pressure and the pore water pressure (or the back-pressure).

## Monotonic Tests

Two series of monotonic tests,  $M$  and  $N$  were conducted on Gangetic silt similar to those carried out by Casagrande and Poulos (1964) on compacted specimens. A total of 13 tests in series  $M$  and 8 tests in series  $N$  were carried out as given below:

(a) Series  $M$  tests: After application of cell pressure (i.e., chamber pressure or all-round pressure or confining pressure) of 500 kPa in one step, back-pressure was applied and the specimen was allowed to saturate for 24 hours. The main purpose of applying back-pressure was

to obtain a low value of initial effective confining stress  $\sigma'_c$  so that the response of specimens could be examined under low  $\sigma'_c$  values. The back-pressure also produced full saturation by dissolving the air voids in the specimen into solution. The specimen was then failed under monotonic loading using an axial strain rate of 4 mm/h.

(b) Series *N* tests: Required cell pressure was applied in one step and the specimen was allowed to saturate in an undrained condition for 6 hours. The cell pressure causes the air voids in the quasi-saturated specimens to be dissolved into solution and the soil behaves like saturated material. The specimen was then failed under monotonic loading using an axial strain rate of 4 mm/h.

### Cyclic Tests

Two series of cyclic load tests, *A* and *B* were conducted on quasi-saturated compacted specimens of Gangetic silt. A total of 5 tests in series *A* and 4 tests in series *B* was conducted. The test procedures in series *A* and *B* tests were quite similar to series *M* and *N* tests, respectively, except that in series *A* and *B* tests, the specimen was subjected to 100 load cycles at a loading frequency of 1 cycles per minute before it was failed under monotonic loading. Slow cyclic tests were preferred because in slow tests, pore pressure measurements are reliable. Loading frequency is known to have no effect over a range of 0.01 to 10 Hz on pore pressure and deformation behavior of the soil (Brown et al. 1975). The total number of load cycles for all tests was chosen as 100 because it is known that the first few cycles are only important to make observations on changes in both the pore pressure and deformation (Wood, 1982). An uniform cell pressure of 700 kPa was used in series *B* tests. Cyclic stress ratio,  $R_f$  is defined as

$$R_f = \frac{q_r}{q_s} \quad (1)$$

where  $q_s$  is the ultimate failure deviator stress in a monotonic undrained compression test and  $q_r$  is the cyclic deviator stress.

Based on the prototype situation, stress-controlled cyclic tests were preferred over strain-controlled tests. A sinusoidal form of loading wave as shown in Fig. 2 was used since it is considered to be nearly representative of the effect of train loading. The subgrade soil below railway formations is subjected to a very low effective confining stress, generally ranging from 5 to 15 kPa depending on the thickness of the formation. However, due to the fluctuations of the measuring system, which were of the order of 2 kPa, tests were conducted at  $\sigma'_c$  values of 20 and 40 kPa (series *A*) so that the results

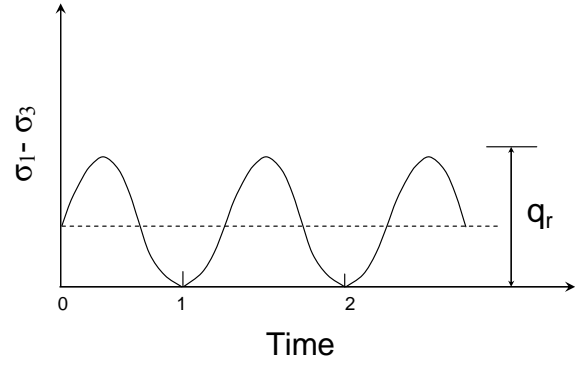


Fig. 2 Sinusoidal loading wave form

could be extrapolated to required confining pressure. The tests in series *B* were carried out at relatively high initial effective confining stresses ranging from 163 to 385 kPa so that the results at high effective confining stresses could be compared with that at low effective confining stresses. This is expected to give a complete picture of the cyclic load behavior of the soil. The initial pore water pressure in series *B* tests varied from 537 to 315 kPa.

### PROCEDURE TO ENSURE QUASI-SATURATED BEHAVIOR

Since series *N* and *B* tests included specimens with varying degrees of saturation and only the pore water pressure was measured in these tests, it is necessary to establish the relevant degree of saturation and cell pressure values above which the quasi-saturated behavior is expected.

Figure 3(a) presents the variation of pore pressure parameter,  $B$  ( $B = \Delta u / \Delta \sigma_3$ , where  $\Delta u$  is the change in pore water pressure due to the application of cell pressure,  $\Delta \sigma_3$ ) with degree of saturation,  $S_r$  for Gangetic silt specimens. For  $S_r$  values less than 0.9, the specimens give the same response almost up to cell pressure of 900 kPa with  $B$ -value approximately equal to 0.2. For  $S_r$  values between 0.90-0.93, though  $B$ -values show a slight increase, still the change in  $B$ -value with cell pressure does not appear to follow any trend. For  $S_r$  values above 0.93,  $B$ -values increase significantly with an increase in either degree of saturation or cell pressure. Based on these data, it is suggested that for  $S_r$  values greater than 0.93 ( $w > \text{OMC} + 1.0\%$ ) and  $B$ -values equal to or greater than 0.4, the soil specimens will exhibit the quasi-saturated behavior. Thus, with the increase in cell pressure to a level that normally exists in engineering problems, the air voids in these specimens will dissolve into solution and the soil will behave like saturated material (Shahu et al., 1999). The measurement of pore water pressure alone will be sufficient for these

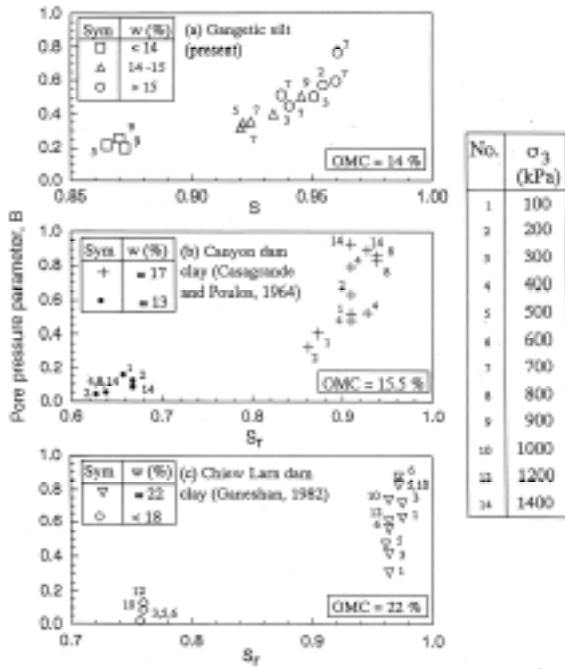


Fig. 3 Variation of pore pressure parameter B with degree of saturation for Gangetic silt

specimens.

Data for Canyon dam clay (having soil properties similar to Gangetic silt) and Chiew Lam dam clay (% finer than 0.002 mm = 53 %;  $I_p = 25-31$ ;  $\gamma_d = 16.95$  kN/m<sup>3</sup>) are presented in Figs. 3b and 3c. For Canyon dam clay (having  $\gamma_d$  values less than that for Gangetic silt), the quasi-saturated behavior is expected for  $S_r$  values greater than 0.9 and  $B$ -values greater than 0.5. Chiew Lam dam clay with higher clay content and plasticity index than Gangetic silt and Canyon dam clay, is expected to show the quasi-saturated behavior for  $S_r$  values greater than 0.95 and  $B$ -values greater than 0.3.

Figure 4 brings out the effect of cell pressure on initial pore water pressure and degree of saturation. The data points represent increase in pore water pressure due to application of total cell pressure in one single step and the dashed lines correspond to increase in pore water pressure due to application of total cell pressure in small increments. Referring to the line for water content,  $w$  equal to 16.6%, it will be seen that at low cell pressure values (less than 250 kPa), the specimen remains essentially partially saturated and the initial pore water pressure increases gradually as the confining stress is increased. Once the cell pressure becomes large enough to completely dissolve the air voids, the specimen becomes fully saturated and the specimen state lies on a line parallel to 1:1 line.

TEST RESULTS AND DISCUSSION

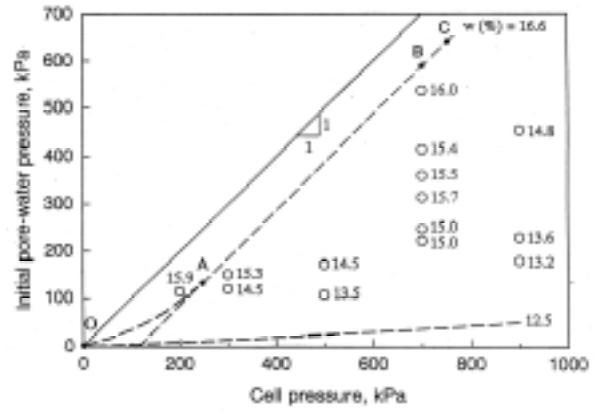


Fig. 4 Cell pressure versus initial pore water pressure

Quasi-Saturated Behavior under Critical State Framework

Critical state soil mechanics provide a rational framework that enables the formulation of a valid constitutive model for saturated resedimented soils in states of effective stress and specific volume. Figs. 5 and 6 show the stress-deformation behavior of quasi-saturated compacted specimens in the general framework of the modified Cam-clay model (Shahu et al., 1999). Recompression line ( $\kappa$ -line), Hvorslev surface and Critical state line in these figures were established as the best-fit lines through a significant number of actual data points.

Virgin consolidation line (VCL) was established using the generalized guidelines given by Yudhbir and Wood (1989). The following critical state parameters were evaluated:  $\lambda = 0.08$ ,  $\kappa = 0.018$  and  $M = 1.31$ .

The physical state of specimens used in series A and B tests is given in Table 1. The specimens in series A became fully saturated due to the application of back-pressure. The  $B$ -value for the specimens in series B tests ranges from 0.45 to 0.77. The initial value of  $S_r$  for these specimens varies between 0.94-0.96 and the range of water content is from OMC + 1.4% to OMC + 2.0%. Hence, as discussed earlier, these specimens are also expected to exhibit quasi-saturated behavior.

The cyclic load behavior of series A and B specimens in critical state framework is shown in Figs. 5 and 6. The initial state of these specimens lie on the recompression line in  $w$  versus  $\ln(p')$  space (Fig. 5). Hyde and Ward (1985) proposed that Hvorslev surface would form an empirically determined failure surface for cyclic effective stress paths for over-consolidated soils. This characteristic is also exhibited by compacted Gangetic silt specimens (Fig. 6). The cyclic effective stress path for tests B3 and B4 that were cycled at  $R_f$  greater than  $R_{TS}$  moved to the Hvorslev surface and further

Table 1 Data for series A and B tests

Test	w (%)	$\gamma_d$ (kN/m)	$S_r$ (%)	$e_0$	$\sigma'_c$ (kPa)	$\frac{(\sigma_1 - \sigma_3)_{max}}{2}$ (kPa)	$\frac{(\sigma'_1 + \sigma'_3)_{max}}{2}$ (kPa)	$q_r$ (kPa)
A1	14.64* 17.00**	18.60	91.34* 100.00**	0.43	22	172	304	50.0
A2	13.75 16.47	18.98	91.96 100.00	0.40	20	212	408	85.0
A3	14.00 16.40	18.77	90.08 100.00	0.41	40	240	440	76.0
A4	13.50 16.87	18.81	87.51 100.00	0.41	40	180	329	100.0
A5	14.20 16.50	18.70	90.21 100.00	0.42	40	222	406	126.0
B1	15.49	18.43	93.74	0.44	340	405	761	150.0
B2	15.71	18.37	94.07	0.44	385	330	615	210.0
B3	15.39	18.60	96.02	0.43	285	345	610	260.0
B4	15.99	18.39	96.08	0.44	163	255	455	160.0

\* Initial value before back pressure saturation; \*\* Final value after the test

application of cyclic loading produced excessive plastic strain indicating failure.

Cumulative Plastic Strain

The term cumulative plastic strain  $\epsilon_p$  is explained in Fig. 7. This term is also referred as permanent strain or irrecoverable strain or simply plastic strain.

Considerable literature related to plastic strain and pore pressure development during cyclic loading of saturated soils and the evaluation of threshold stress is available (Wood, 1982). The relationship between cumulative plastic strain,  $\epsilon_p$  and number of load cycles,  $N$  is essential to predict the time period for maintenance

cycle of pavements and railway tracks. Li and Selig (1996) used the following linear model for this relationship for fine grained soils:

$$\epsilon_p = c N^d \tag{2}$$

where  $c$  and  $d$  are constants. The Dutch Office for Research and Experiments, International Union of Railways, ORE (1970) proposed the following relationship for London clay:

$$\log(\epsilon_p) = 1.39 \epsilon_e - 1.74 + 0.622 \log N \tag{3}$$

where  $\epsilon_e$  is average elastic strain in percent. Hyde and Brown (1976) proposed the following relationship between plastic strain rate per unit time,  $\dot{\epsilon}_p$  and time,  $T$  based on cyclic triaxial tests on remolded silty clay:

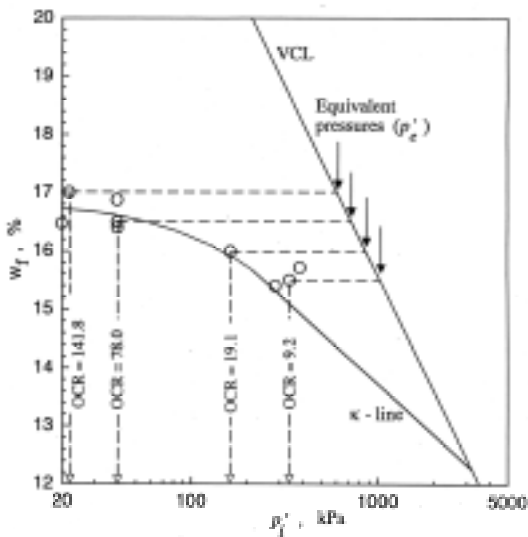


Fig. 5  $w_f$  versus  $p'_i$  relationship

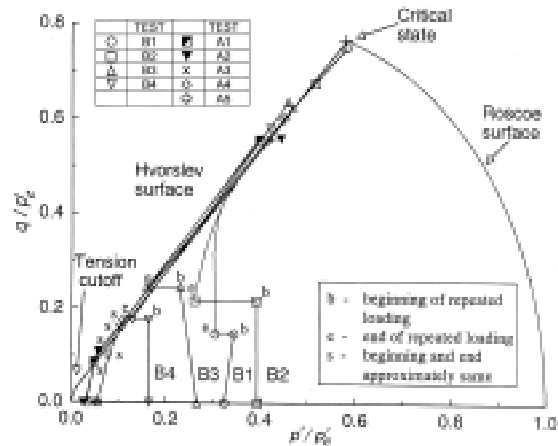


Fig. 6  $q/p'_e$  versus  $p'/p'_e$  relationship for Gangetic silt

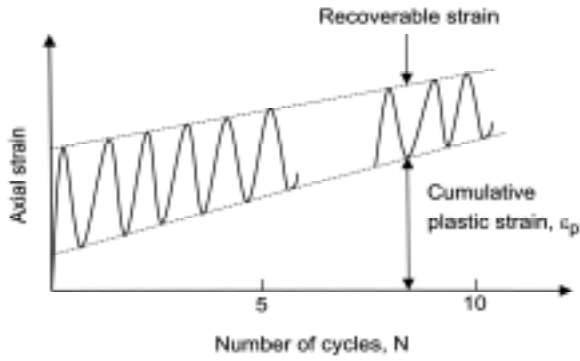


Fig. 7 Explanation of the term cumulative plastic strain

$$\log \dot{\epsilon}_p = C - D \log T \quad (4)$$

where  $C$  is the logarithm of strain rate at unit time and  $D$  is the strain rate decay constant. Several other researchers have also presented the relationship between  $\epsilon_p$  and  $N$  independently on a range of soil types in the saturated state (for example, see Wilson and Greenwood, 1974; ORE, 1983; Hyde and Ward, 1985).

Figures 8 and 9 show the relationship between  $\epsilon_p$  and number of load cycles,  $N$  in cyclic triaxial tests for Gangetic silt. The following trends were observed. First,

cumulative plastic strain increases with cyclic deviator stress (or  $R_f$ ) for the same number of load cycles. Second, for the tests conducted at low cyclic stress levels, a stable deformation behavior is observed, and after a certain number of load cycles, very small increase in cumulative plastic strain is obtained with further increase in number of load cycles. For example, for tests A1, A3 and B1,  $\epsilon_p$  values attain maximum at  $N$  ranging from 20 to 60 after which practically no more increase in plastic deformation occurs. Third, for tests conducted at a relatively higher cyclic stresses,  $\epsilon_p$  values either show a linear increase (Tests A2 and B2) with number of load cycles or exhibit a bilinear behavior (Tests A5, B3 and B4) in a log-log plot with the second slope being greater than the first slope. The above trends were also observed by ORE (1983) for cyclic triaxial tests carried out on stiff undisturbed specimens of Boulder clay ( $I_p = 17$ ) and Keuper Marl ( $I_p = 15$ ) with an initial effective confining stress,  $\sigma'_c$  of 35 kPa and a loading frequency of 30 cycles per minute (Fig. 10).

Since a railroad track passes through a number of soil types, it is useful to propose a simple relationship for prediction of cumulative plastic strain with number of load cycles. On the basis of results presented above, the following generalized bilinear log-log model is proposed for this purpose (Fig. 11):

$$\log(\epsilon_p) = C_p + D_p \log(N_1) + E_p \log(N_2/N_s) \quad (5)$$

where for  $N \leq N_s$ ,  $N_1 = N$  and  $N_2/N_s = 1$   
and, for  $N > N_s$ ,  $N_1 = N_s$  and  $N_2 = N$

In this equation,  $C_p$  is the value of  $\log(\epsilon_p)$  at  $N$  equal to 1;  $D_p$  and  $E_p$  are the first and second gradients of the bilinear log-log plot between  $\epsilon_p$  and  $N$  respectively; and  $N_s$  is the value of  $N$  where the change in gradient from  $D_p$  to  $E_p$  occurs. Curves back-fitted on experimental data

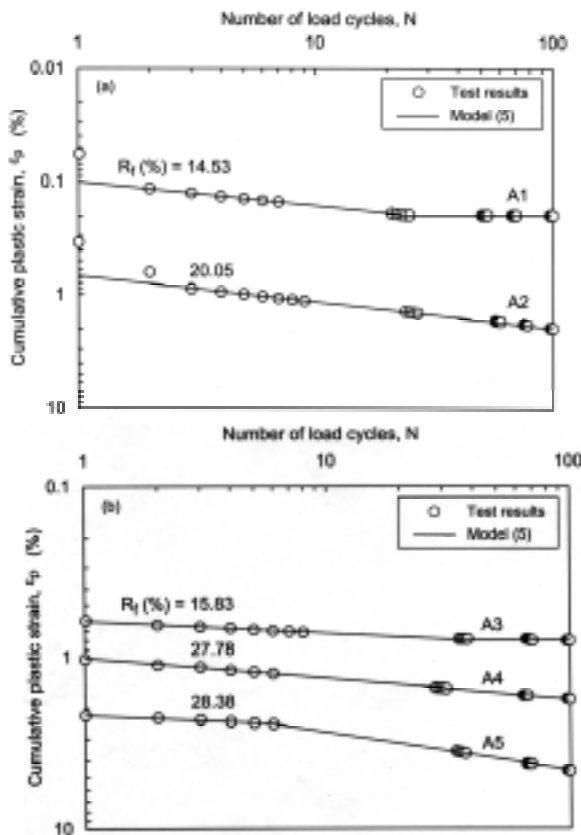


Fig. 8  $\epsilon_p$  versus  $N$  relationship for back-saturated Gangetic silt specimens: (a)  $\sigma'_c = 20-22$  kPa; (b)  $\sigma'_c = 40$  kPa

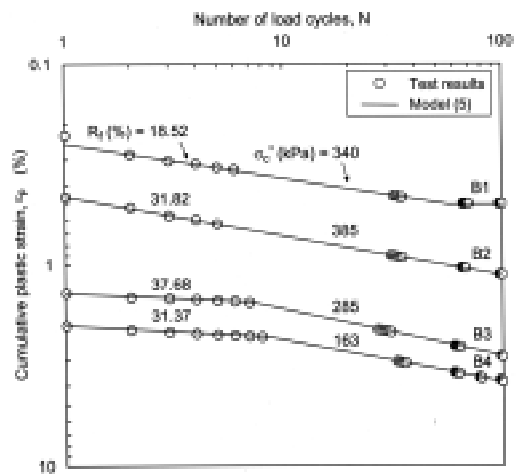


Fig. 9  $\epsilon_p$  versus  $N$  relationship for quasi-saturated Gangetic silt specimens with high  $\sigma'_c$  values

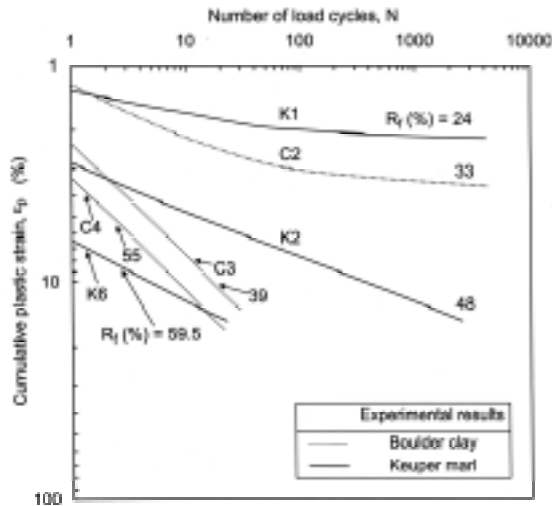


Fig. 10  $\epsilon_p$  versus  $N$  relationship for stiff undisturbed Keuper marl and Boulder clay specimens (ORE, 1983)

using this model (Eq. 5) are shown in Figs. 8 and 9 and the model parameters are given in Table 2.

The data from the Wilson and Greenwood (1974) is plotted in Fig. 12. The bilinear model (Eq. 5) represents the test data quite accurately. Inadequacy of a linear model of the type given by Eq. (2) (Li and Selig, 1996) to represent cumulative plastic strain data is clearly brought out in this figure. Moreover, the linear model (Eq. 2) is a particular case of the bilinear model (Eq. 5) with  $D_p = E_p$ . Thus, all data modelled by Eq. (2) will also be successfully represented by Eq. (5). The bilinear model also has an important physical significance. Three mechanisms are mainly responsible for the cumulative plastic deformation of fine-grained soils under repeated loading. They are cumulative compaction, cumulative consolidation and cumulative plastic shear strain mechanisms. From Figs. 8 to 10 and Fig. 12, it will be seen that for cyclic stresses less than a certain stress

Table 2. Value of coefficients in plastic strain model (Eq. 5)

Test	$R_f$ (%)	$\sigma'_c$ (kPa)	$C_p$ (%)	$D_p$ (%)	$E_p$ (%)	$N_s$	$R_{TS}$ (%)
Compacted Gangetic Silt. $I_p = 14$ .							
A1	14.53	22	-1.000	0.209	0.000	25	20.0
A2	20.05	20	-0.150	0.220	-	OOS*	
A3	15.83	40	-0.215	0.078	0.000	33	
A4	27.78	40	0.013	-	0.117	OOS	28.3
A5	28.38	40	0.342	0.072	0.207	06	
B1	18.52	340	-0.593	0.167	0.000	56	
B2	31.82	385	-0.337	-	0.195	OOS	31.8
B3	37.68	285	0.146	0.058	0.234	07	
B4	31.37	163	0.305	0.064	0.205	08	
NC Undisturbed Lacustrine Clay. $I_p = 14$ . Wilson and Greenwood (1974).							
L1	30.00	350	-1.108	0.032	-	OOS	
L2	59.00	350	-0.740	0.111	0.462	26	59.0
L3	80.00	350	-0.430	0.083	0.568	05	
Stiff Undisturbed Boulder Clay. $I_p = 17$ . ORE (1983).							
C1	27.80	35	-0.022	0.139	0.052	40	
C2	33.00	35	0.086	0.244	0.024	40	39.0
C3	39.00	35	0.371	-	0.520	OOS	
C4	55.00	35	0.544	-	0.520	OOS	
Stiff Undisturbed Keuper Marl. $I_p = 15$ . ORE (1983).							
K1	24.00	35	0.121	0.105	0.011	52	
K2	48.00	35	0.477	-	0.208	OOS	
K3	50.00	35	0.560	-	0.272	OOS	48.0
K4	55.00	35	0.690	-	0.292	OOS	
K5	52.30	35	0.707	-	0.342	OOS	
K6	59.50	35	0.810	-	0.280	OOS	
NC Undisturbed Newfield Clay. $I_p = (17-19)$ . Sangrey (1968).							
S1	49.00	393	-0.300	0.176	-	OOS	-
S2	80.00	393	0.342	0.265	0.820	02	62.0
S3	89.00	393	0.467	-	0.560	OOS	-

\*OOS - Only One Slope.

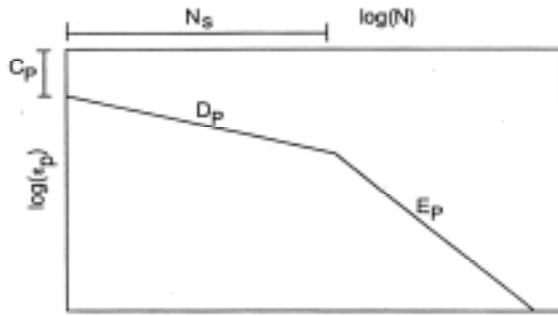


Fig. 11 Definition of model parameters

level, namely, threshold stress (Table 2),  $E_p$  values are either less than  $D_p$  values or equal to zero and a stable deformation behavior is indicated representative of cumulative compaction mechanism. On the other hand for cyclic stresses greater than or equal to threshold stress,  $E_p$  values are either equal or greater than  $D_p$  values indicating cumulative plastic shear strain mechanism.

Evaluation of Threshold Stress

To avoid excessive track maintenance, the induced stresses on the subgrade surface due to traffic loading should be less than the threshold stress of the subgrade soil. Since this criterion generally forms the basis of a rational track design, the knowledge of the threshold stress of the subgrade soil is essential for proper track design. Larew and Leonards (1962) first indicated the existence of threshold stress on the basis of total stress cyclic tests. Later, based on effective stress tests on a saturated clay, Sangrey (1968) confirmed that there exists a critical level of repeated stress ( $CLRS$ ) such that when the cyclic stress level is above  $CLRS$ , plastic deformation is non-terminating.  $CLRS$  is commonly known as threshold stress and is usually smaller than the static strength of the soil under monotonic loading. Subsequently other researchers also evaluated the

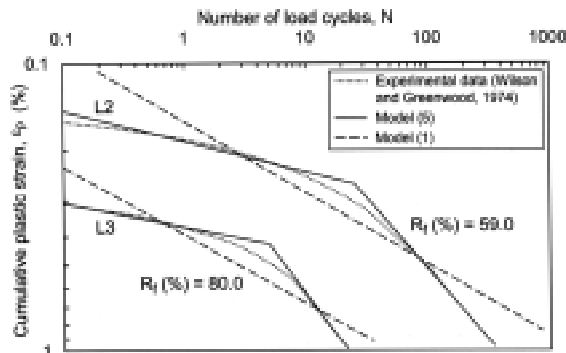


Fig. 12  $\epsilon_p$  versus  $N$  relation for normally consolidated lacustrine clay (Wilson and Greenwood, 1974)

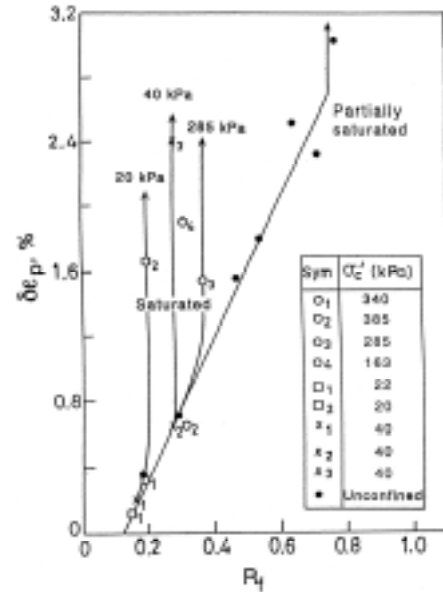


Fig. 13 Rise in plastic strain during 100 load cycles versus  $R_f$

threshold stress for cohesive soils under saturated conditions (e.g., ORE, 1970; Sangrey et al., 1978; ORE, 1983).

In past, threshold stress has been evaluated by different researchers using different procedures and definitions. For example, ORE (1970) defined threshold stress as the maximum stress that does not cause cumulative plastic strain greater than 10% in 1000 cycles in cyclic triaxial tests. Sangrey (1968) evaluated the threshold stress by observing the movement of effective stress path with the increase in pore water pressure in cyclic triaxial tests and using equilibrium line concept. In general, threshold stress is evaluated either by using plastic strain criterion or by using pore pressure generation criterion. In this section, threshold stress of quasi-saturated Gangetic silt is evaluated by using both plastic strain and pore pressure generation criteria using test data obtained from cyclic triaxial tests. Guidelines are given for the evaluation of threshold stress for a variety of soils at low and relatively high effective confining stresses.

Plastic strain criterion

Figure 13 shows the test data in terms of incremental values of  $\epsilon_p$  during 100 load cycles ( $\Delta\epsilon_p$ ) as related to  $R_f$  for different  $\sigma'_c$  values. The value of  $R_f$  at which a sudden increase in the incremental plastic strain occurs, may be taken as a measure of threshold stress ratio. For example, for tests with  $\sigma'_c = 20-22$  kPa (series A tests),  $\Delta\epsilon_p$  values show a sudden increase for  $R_f = 20.0\%$ . This  $R_f$  value is representative of threshold stress ratio,  $R_{TS}$  for compacted Gangetic silt. The corresponding values of



$R_{TS}$  for  $\sigma'_c = 40$  kPa and 285 kPa have been evaluated as 28.3 % and 31.8 %, respectively. In a similar manner,  $R_{TS}$  values for other soils are also evaluated and listed in Table 2.

**Pore pressure criterion**

Sangrey (1968) was first to evaluate the threshold stress from pore pressure generation criterion using equilibrium line concept. Sangrey et al. (1978) later confirmed the existence of an equilibrium line for a variety of saturated soils. Roughly speaking, an equilibrium line joins the locus of end points of cyclic effective stress paths that have reached equilibrium with the failure envelope. The end point of the equilibrium line on the failure envelope is a good measure of the threshold stress.

While the total change in pore water pressure during 100 load cycles for series A tests was of the order of 2-5 kPa, the fluctuations of the measuring system were also of the same order. Hence, the pore water pressure data for series A tests were not used for threshold stress determination. For series B tests, the pore water pressure response during 100 load cycles is given in Fig. 14.

The movement of normalized effective stress paths during 100 load cycles is indicated by an arrow in Fig. 15 for series B tests. The shaded portion in this figure indicates the range of normalized effective stress paths for comparable monotonic tests from series N. Point A is the end point of effective stress path of normally consolidated specimens on  $k'_f$  line and is termed as the critical stress level on failure line. No stress state can exist below this level on the failure line.

The end points of tests B1 and B2 are joined with the failure line to determine the equilibrium line (Fig. 15). The equilibrium line meets the failure line at point A and hence, the stress level corresponding to point A is representative of  $R_{TS}$ . To evaluate this value of  $R_{TS}$ , an inset showing the variation of  $(\Delta u_{cyc} / \sigma'_c)$  with  $R_f$  is plotted, where  $\Delta u_{cyc}$  is the increase in pore water pressure during 100 load cycles. A smooth curve passing

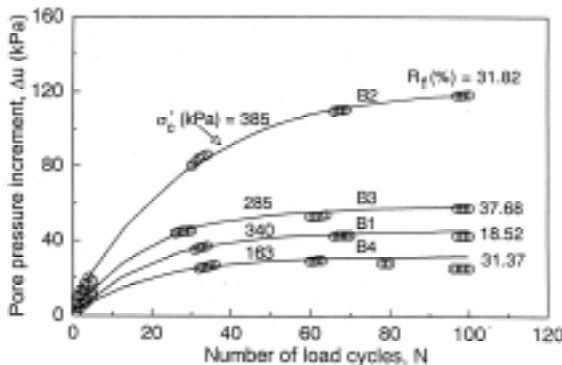


Fig. 14 Pore pressure rise with number of load cycles for specimens with high  $\sigma'_c$  values

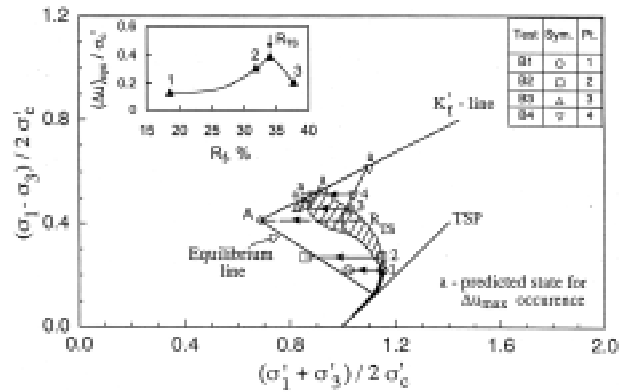


Fig. 15 Normalized stress path for specimens with high  $\epsilon$  values

through the data points touches the value of  $(\Delta u_{cyc} / \sigma'_c)$  corresponding to point A at  $R_f$  equal to 33.8 % and this value of  $R_f$  is representative of  $R_{TS}$ . Considering the normalized procedure used in this study involving limited number of samples tested at a range of  $\sigma'_c$  values ( $\sigma'_c = 285$ -385 kPa), this value is quite comparable with  $R_f$  equal to 31.8 % obtained from plastic strain criterion (Table 2).

**Guidelines for prediction of threshold stress**

For quick estimates, it is useful to work out some empirical relationships between  $R_{TS}$  and simple soil indices. Sangrey et al. (1978) have proposed a relationship between  $R_{TS}$  and soil compressibility factor,  $\kappa / (1 + e_0)$  where  $e_0$  is the initial void ratio of the soil. However  $\kappa$  determination poses certain difficulties and it needs to be determined in the range of changes in  $\sigma'_c$  during cyclic loading. Since compressibility of soil depends on plasticity index  $I_p$ , a relationship between  $R_{TS}$  and  $I_p$  is attempted here. Easy determination of  $I_p$  as compared to  $\kappa$  is a desirable feature of the proposed inter-relationship. Figure 16 presents available test data

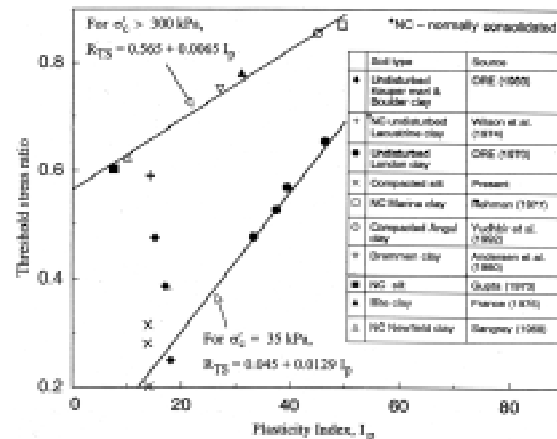


Fig. 16 Threshold stress ratio versus plasticity index relationship

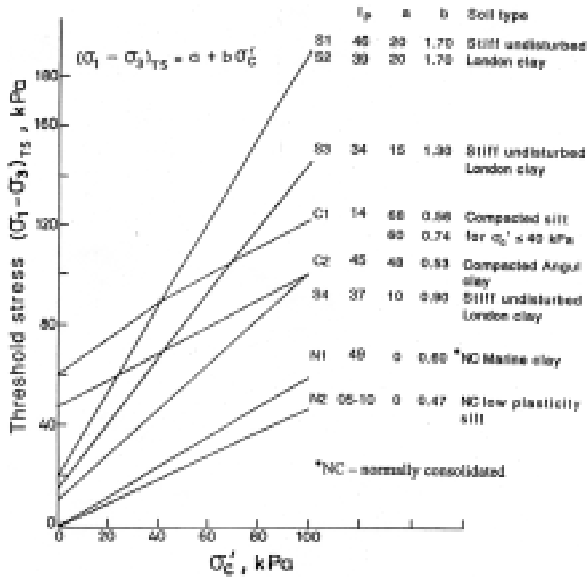


Fig. 17 Threshold stress versus  $\sigma'_c$  relationship

for a variety of soils (compacted, stiff, normally consolidated, etc.) at low and relatively high effective confining stresses. The following empirical relationships between  $R_{TS}$  and plasticity index,  $I_p$  are suggested as guidelines to estimate  $R_{TS}$ :

For  $\sigma'_c > 300$  kPa,

$$R_{TS} = 0.565 + 0.0065 I_p \quad (6)$$

and, for  $\sigma'_c = 35$  kPa,

$$R_{TS} = 0.045 + 0.0129 I_p \quad (7)$$

However, the value of  $\sigma'_c$  required for compacted low  $I_p$  soils to follow Eq. (6) is expected to be much higher than 300 kPa. While Eq. (6) is useful for predicting dynamic bearing capacity of soils, Eq. (7) is relevant for estimating threshold stress for railway formation design.

However, since  $\sigma'_c$  values relevant to railway formation problems are smaller than 35 kPa, the variation of threshold stress with  $\sigma'_c$  was also examined. The threshold stress for compacted Gangetic silt samples at  $\sigma'_c$  values of 20, 40 and 285 kPa was obtained from Fig. 13. The following straight line relationship for evaluation of threshold stress is suggested at low  $\sigma'_c$  values (Fig. 17):

$$(\sigma_1 - \sigma_3)_{TS} = a + b \sigma'_c \quad (8)$$

where  $(\sigma_1 - \sigma_3)_{TS}$  is the threshold stress of soil in terms of deviator stress; and, coefficients  $a$  and  $b$  are the intercept and slope of the line in  $(\sigma_1 - \sigma_3)_{TS}$  vs.  $\sigma'_c$  plot. The relationship between threshold stress and  $\sigma'_c$  for a variety of soil types, namely, stiff undisturbed London clay (ORE, 1970), compacted Angul clay

(Yudhbir et al., 1992), normally consolidated marine clay (Rehman, 1977), and normally consolidated low plasticity silt (Gupta, 1973) was also evaluated. The results obtained for all these soils at low effective confining stresses are also depicted in Fig. 17.

## CONCLUSIONS

Stress-deformation behavior of quasi-saturated compacted specimens has been successfully interpreted in the general framework of the modified Cam-clay model. The cyclic undrained behavior of quasi-saturated specimens has been then interpreted using this critical state framework. Pore pressures generated during cyclic loading tend to move the effective stress path towards Hvorslev surface and further application of cyclic loading produces excessive plastic strain indicating failure.

Cyclic stress level in relation to threshold stress determines whether plastic strains will stabilize, or lead to excessive deformation and eventual failure in the quasi-saturated compacted soil. A generalized bilinear log-log relationship is proposed for the prediction of cumulative plastic strain with number of load cycles. This relationship is also found to predict the test data for saturated fine grained soils satisfactorily.

A clear-cut value of threshold stress ratio was obtained for the quasi-saturated compacted silty clay specimens. This value of threshold stress ratio was evaluated using both plastic strain development and pore pressure generation criteria. For quick estimation of threshold stress ratio  $R_{TS}$ , linear relationships between  $R_{TS}$  and plasticity index  $I_p$  with varying slopes (depending upon confining stress level) are proposed for a variety of soil types (e.g., compacted, stiff, normally consolidated). Linear relationships are also suggested between threshold stress and confining stress at low effective stress ranges for railway formation design.

## REFERENCES

- Andersen, K.H. (1980). Cyclic and static laboratory tests on Drammen clay. Norwegian Geotech. Inst. Pub., 131:1-31.
- Brown, S.F. (1996). Soil Mechanics in pavement engineering. 36th Rankine Lecture. Geotechnique, 46:383-426.
- Brown, S.F., Lashine, A.K.F. and Hyde, A.F.L. (1975). Repeated load triaxial testing of a silty clay. Geotechnique, 25:95-114.

- Casagrande, A. and Poulos, J. (1964). Fourth progress report on investigation of stress, deformation and strength characteristics of compacted clays. A research project sponsored by 'The Waterways Experiment Station' in co-operation with Harvard University, Cambridge, Massachusetts.
- Cruz, P.T. (1985). Peculiarities of tropical lateritic and saprolitic soils used as construction materials: Selection, control and acceptance criteria — Dams. Progress Report of Committee on tropical Lateritic and Saprolitic soils, Brazilian Society of Soil Mechanics: 275-327.
- France, J.W. (1976). An investigation of the effects of the drainage on the repeated load behavior of soils. MS thesis, Cornell Univ. at Ithaca, USA.
- Ganeshan, V. (1982). Strength and collapse characteristics of compacted residual soils. ME thesis, Asian Inst. of Tech., Bangkok, Thailand.
- Gupta, S.K. (1973). Undrained behavior of a silt from Indo - Gangetic alluvium. MTech thesis, Indian Inst. of Tech., Kanpur, India.
- Hyde, A.F.L. and Brown, S.F. (1976). The plastic deformation of a silty clay under creep and repeated loading. *Geotechnique*, 26:173-184.
- Hyde, A.F.L. and Ward, S.F. (1985). A pore pressure and stability model for a silty clay under repeated loading. *Geotechnique*, 35:113-125.
- Larew, H.G. and Leonards, G.A. (1962). A strength criterion for repeated loading. *Proc. Highway Research Board*, 41:529-556.
- Li, D. and Selig, E.T. (1996). Cumulative plastic deformation for fine-grained subgrade soils. *Journal of Geotechnical Engineering*, 122:1006-13.
- ORE (1970). Question D71: Stresses in the rails, the ballast and in the formations resulting from traffic loads. Report 12: Repeated loading of clay and track foundation design. Report D71/RP12, Office for Research and Experiments, International Union of Railways, Utrecht, Netherlands.
- ORE (1983). Question D 117: Optimum adoption of the conventional track to future traffic. Report 25: The behavior of the track bed structure under repeated loading (Tests at Vienna arsenal and Derby). Report D117/RP25, Office for Research and Experiments, International Union of Railways, Utrecht, Netherlands.
- Rehman, M.S. (1977). Undrained behavior of saturated normally consolidated clay under repeated loading. MTech thesis, Indian Inst. of Tech., Kanpur, India.
- Sangrey, D.A. (1968). The behavior of soils subjected to the repeated loading. Ph. D. thesis, Cornell Univ., Ithaca, USA.
- Sangrey, D.A., Castro, G., Poulos, S.J. and France, J.W. (1978). Cyclic loading of sands, silts and clays. *Proc. specialty conf. on Earthquake Engineering and soil dynamics*, ASCE, Pasadena: 836-851.
- Shahu, J.T., Yudhbir and Kameswara Rao, N.S.V. (1999). Effective stress behavior of quasi-saturated compacted cohesive soils. *Journal of Geotechnical and Geoenvironmental Engineering*, ASCE, 124:322-329.
- Vanapalli, S.K., Fredlund, D.G., Pufahl, D.E. and Clifton, A.W. (1996). Model for the prediction of shear strength with respect to soil suction. *Canadian Geotech. J.*, 33:379-392.
- Wilson, N.E. and Greenwood, J. R. (1974). Pore pressures and strains after repeated loading of saturated clay. *Canadian Geotech. J.*, 11:269-277.
- Wood, D.M. (1982). Laboratory investigations of the behavior of soils under cyclic loading: A review. In: G. N. Pande and O. C. Zienkiewicz., eds., *Soil Mechanics - Transient and Cyclic loads*, John Wiley and Sons: 513-582.
- Yudhbir, Kameswara Rao, N.S.V. and Shahu, J.T. (1992). Design of track formation at Angul for Nalco (Orissa). Dept. of Civil Engg., IIT Kanpur, India.
- Yudhbir and Wood, D.M. (1989). Recent developments in laboratory strength and deformation testing. General report, 12<sup>th</sup> International Conference on Soil Mechanics and Foundation Engineering, Rio de Janeiro, Brazil 4: 2303-2338.